

PLANAR SINGLE LOOP SQUARE SPIRAL RING RESONATOR FOR NEAR FIELD NANO LAYER DETECTION

Nadeem Naeem^{1*}, Sajida Parveen¹, Alyani Ismail², Anwer sabah Mekki³

¹Faculty of Electrical, Electronics and Computer Systems Engineering, Quaid-e-Awam University of Engineering, Sci. & Technology, Nawabshah, Pakistan

²Research Centre of Excellence For Wireless And Photonics Network, Universiti Putra Malaysia, Serdang, Selangor, Malaysia

³Sensor technology Engineering, Institut teknologi maju (ITMA), Universiti Putra Malaysia, Serdang, Selangor, Malaysia

*Corresponding author: nadeemnaeem@yahoo.com

ABSTRACT: *Metamaterials are artificially created sub wavelength structures that attain electromagnetic properties from electrically small metal embedded structures known as split ring resonators and single conducting spiral loops. The structural and functional flexibility presented in the metamaterials have open doors of innumerable applications for researchers and sensing small analytes over a wide frequency range is one of them. The sensor reported in the paper is made up of a single loop of conducting strip exhibits left handedness at terahertz frequency and it can sense the presence of the nano layers having biological and chemical properties. The presence of layers is sensed in terms of shifting of resonance frequency. The reported structure of sensor is made up of single loop of copper conducting metal strips that are arranged on a single side of the base material. Transmission and reflection spectra of this unit cell are simulated using the commercially available 3D EM simulation software. The obtained results clearly showed that the sensor can detect presence of nano layers thus making it quite useful substitute to the ordinary split ring resonators in sensing applications.*

Keywords—Metamaterial; spiral ring; terahertz, nano-layers

INTRODUCTION

The theory of metamaterials was theoretically advised by Pendry in the year of 1999 [1]. The early experimental demonstrations were carried out by Shelby [2]. Such metamaterial based micro structures are the materials that inherit their electromagnetic characteristics from nature. These materials can attain negative values of permittivity and permeability over a certain frequency band by using the combination of periodic arrays of split ring resonators (SRR) and transmission wires [3].

Split ring resonators have appeared in number of geometrical shapes and their arrays because of the flexibility in design and easy implementation. Due to this reason, countless structures are reported in the literature demonstrating the usage of split ring resonators for different frequencies. Few of the recently reported shapes are s-shape resonators [4], omega resonators [5], v-shape resonators [6], hexagon shape [7] and triangular shape [8].

Among all of the resonators, one of the structure type in which the split ring is made up of using single loops of conducting metal is called spiral resonators [9] are reported for left-handed metamaterial applications. There are various spiral resonators are reported in the open literature. Such metamaterial resonators with double negative index property have attracted the research interest particularly for those structures, which are designed to operate in terahertz frequency band for various scientific biomedical applications [10].

The single loop structure exhibits double negative properties in terahertz (THz) frequency. The dimensions of the resonator are smaller than the structure reported in [11, 12]. Such small dimensions enable the resonator (sensor) to operate at higher frequencies. The simulated scattering parameters are used for the retrieval of refractive index, effective permittivity and permeability.

The metamaterials functional and scalable materials that are attributed for being having high spectral capability and thus they can perform well in sensing applications way beyond the

conventional sensors can perform. Metamaterials can detect much smaller objects with dimensions smaller than 100 nanometer, such objects are difficult to get detected by the traditional sensors.

So far, these sensors are designed to wavelengths of visible spectrum but still they are best suited for biomedical and human interaction (safety and security) related sensing applications because of the non ionizing properties of terahertz (THz) frequency.

Terahertz frequency is ranged from 0.1 to 10 THz on frequency spectrum. This frequency band is partially explored due to the fact that all most all naturally occurred sensors have decrease down their functions. Such unexplored scientific gap can only be filled by tiny metamaterials because of their custom-made features that enable terahertz operated metamaterials to be a successful contender for present and next generation research [13].

The boost in designing of terahertz metamaterials has further opened its role in sensing. This is obvious that terahertz metamaterials can find their way in current and future sensing applications in the fields of medicine, astronomy, chemistry and physics.

MATERIAL AND METHODS

Fig 1 shows the dimensions of schematic diagram of the cell structure. This triangular shaped SRR structure is designed with copper strips having the thickness of 0.018 micron and the strip width is $w=0.5$ micron. Spacing between strips is $s=0.5$ micron. The structure is simulated over a 0.5micron thick polyimide substrate with the relative permittivity of 3.5 and permeability of 1. Thinner and low permittivity substrate is arranged in order to minimize loses. Overall cell is dimensioned $10 \times 10 \times 0.5 = 50$ cubic microns. Such dimensions are smaller than reported resonators at terahertz frequency with extremely thin sample layers that are tested on the split gaps on the sensor's surface. The electrical size of resonator is calculated through [14], which is 14.142 micron.

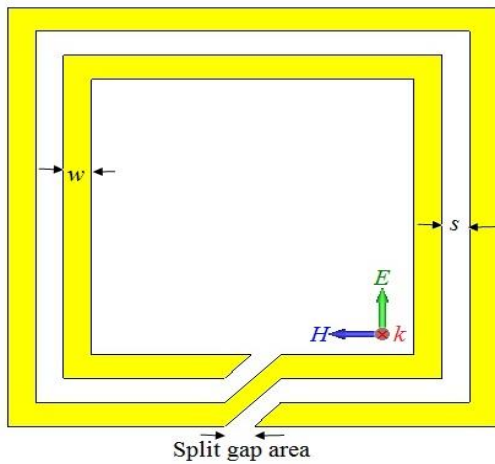


Fig 1. Structure of sensor [10-11].

The resonant structure is simulated using free space environment excited by the electromagnetic wave with propagation vector (*k*) in *z* direction where as the electric field vector (*E*) is aligned in *y* direction and magnetic field vector (*H*) is in *x* direction. The sensor exhibit surface electric field at the split gaps as shown in Fig 2. The concentration of electric field is due to the capacitive effect produced at the split area. This field can also be observed between conducting loops. Tuning the split area surely changes the effect of the field on the sensor’s e surface thereby chaning response of sensor.

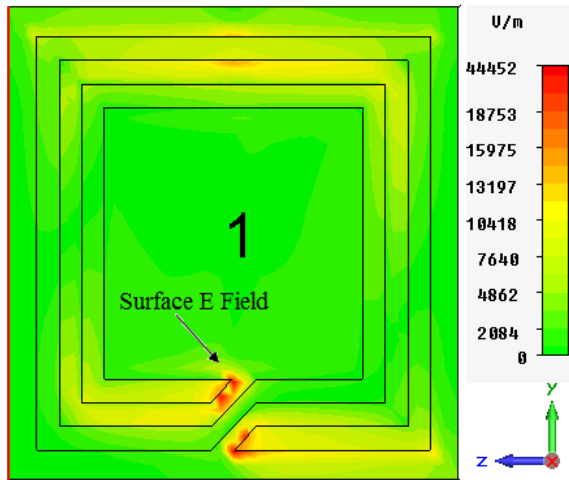


Fig 2. Electric field intensity on the surface of the resonator.

The conducting loops also cause surface electric field so it should be considered that this electric field doesnot responsible to the overall change in the sensor’s behavior. Larger coverage will result in further change. To arrange the nano layers on the sensor’s surface, the split area is commonly selected in order to observe the frequency shifts. This is due to the fact that split gaps serve as highly capacitive regions that are responsible to cause change in the transmission as electric field is disturbed by the application of the thin dielectric layers on its surface.

S-parameters of the unit cell are calculated in order to observe its physical properties. Effective parameters are extracted from a simplified method reported in [15]. The index of refraction (*n*) and wave impedance are calculated using equation (1) and (2). The negative refraction appears at the frequency of resonance. This refraction can be observed in Fig 3, according to which, the real part of the refraction index reveals the left-handedness on perticular region of resonance. The negativeness of refraction resonance is observed from 7.5 to 10 THz.

$$z = \sqrt{\frac{(1 + S_{11})^2 - S_{21}^2}{(1 - S_{11})^2 - S_{21}^2}} \tag{1}$$

where *z* indicates wave impedance

$$n = \frac{1}{kd} \cos^{-1} \left[\frac{1}{2S_{21}} (1 - S_{11}^2 + S_{21}^2) \right] \tag{2}$$

where $k=\omega/c$ is the propagation vector, ω is frequency in radian, *c* is the speed of light and *d* is the unit cell slab thickness.

The real part of the refractive index of the sensor showed negative values at the location on frequency domain where the electromagnetic resonance occurred at 7.5 THz. The negativeness existed up to the frequency of 9.9THz. whereas, the imaginary part showed up with near to zero values. Such situation may be regarded here as refractive index when there is no nano layer deposited on the surface of sensor. It can be observed in Fig 3 that the index is further shifted from the region of actual resonance as the nano layers (with unchanged dielectric constant) are arranged onto the surface. The values of shifting refractive index remained same without any variations. Further shifting in index cause higher shifts in frequency due to the presence of thin nano layers showing the sensitensess of the sensor. Since, the proposed sensor behaves as a double negative structure (in which permittivity and permeability is negative) and the refractive index is interrelated with permittivity and permaeability of the sensor, the phenomena of shifting the resonant frequency can be expected.

Electric permittivity of spiral resonator is calculated next using equation (3).

$$\epsilon = n / z \tag{3}$$

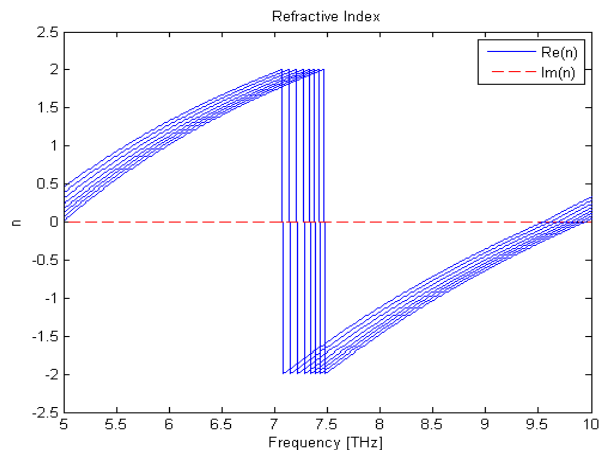


Fig 3. negative index of refraction.

The real part of complex permittivity and permeability of the resonator goes negative at exactly on the negative refraction of index where the resonance occurs and stays negative upto upper boundary of terahertz regime. Where as implication of imaginary values are considered as loss term. The losses are minimized with incorporating most possible thin substrate as a base material upon which, the sensor is arranged. If the thickness of substrate increases, the losses are also get increased at higher frequencies. The effect of negative effective permittivity and permeability is illustrated in Fig 4 and Fig 5. The first values was observed at the resonant frequency, which may also be regarded as unloaded permittivity of the sensor. This effective value of electric permittivity exhibits higher than permeability. This is because of perpendicular incidence of the excitation wave and parallel polarization of electricfield component during simulations.

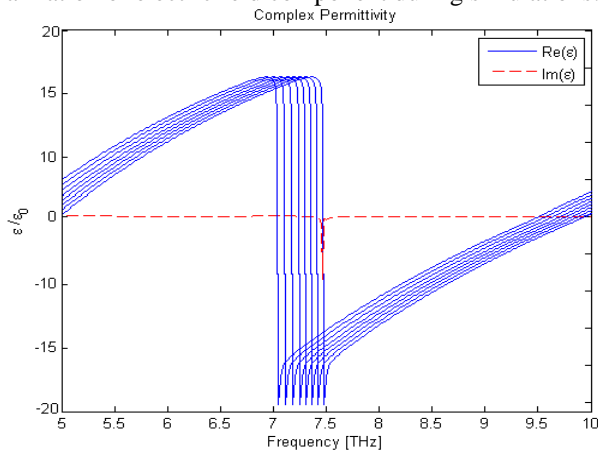


Fig 4. Effective negative permittivity.

The deposition of nanolayer causes the shifts in effective permeability with positive imaginary and negative real parts of the complex quantity. The equivalent capacitance effect decreases due to the interruption in the surface electric field distribution that is localized around gap areas and between the loops of the sensor. As this effect gets stronger, the resonant frequency shifts down to lower values. The magnetic permeability is obtained with the help of equation (4).

$$\mu = n * z \tag{4}$$

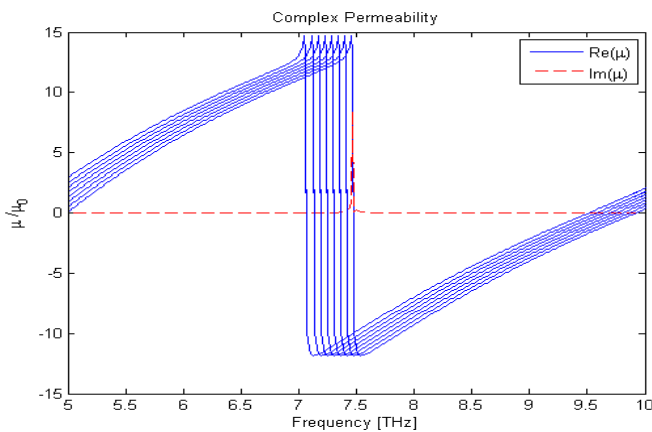


Fig 5. Effective negative permeability

RESULTS AND DISCUSSION

The obvious phenomenon that can be observed in Fig 6 is the shift in the resonant frequency. There is no shift in transmission at the first instance. This is due to the fact that sensor is tested with no nano layer deposition on to the surface.

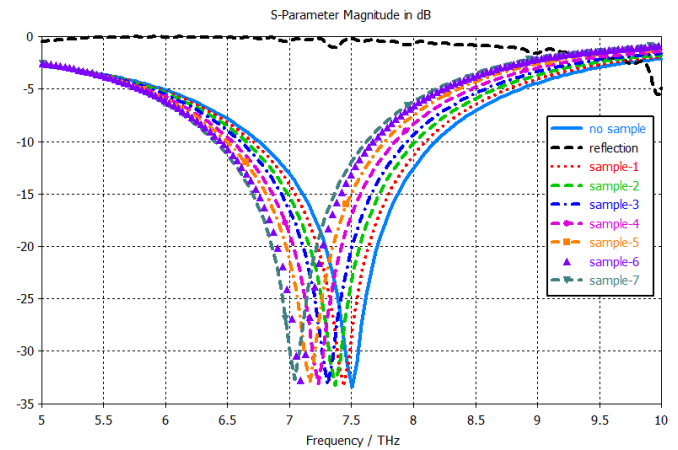


Fig 6. Frequency shift at the resonance under loading conditions.

After that the transmission (S_{21} component) is decreased with deposition of the nano layers. The resonant frequency shifts down itself at lower microwave frequencies as the sensor is loaded with higher permittivity of sample materials. The dielectric constant of the nano layers representing bio samples widely varies because of the layer thicknesses and the water contents present in them. The S_{21} and S_{11} denote the transmission and reflection coefficients, respectively. Least values of the dielectric constants of nano layers are used for testing purpose. Keeping such variation in focus, the nano layers with minimum dielectric constants were tested. The summary of frequency shift is shown in Fig 7.

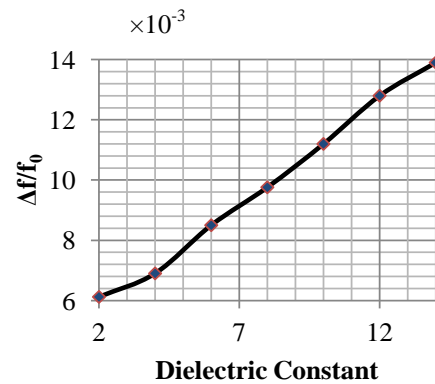


Fig 7. Frequency shifts with changing dielectric constants of nano layers.

The tasting was divided into two portions. The thickness of the nano layer was retained constant in the first part of the experiment and the dielectric constants were changed every time during the simulation. The second portion of experiments involved the changing thickness of the nano layer while the dielectric constant remained unchanged. The dip in transmission resonance upon loading of different samples showing the sensing capability to every loaded tiny

nano layer. Under testing conditions, the split gap areas of spiral rings that are bit sensitive to any surface change.

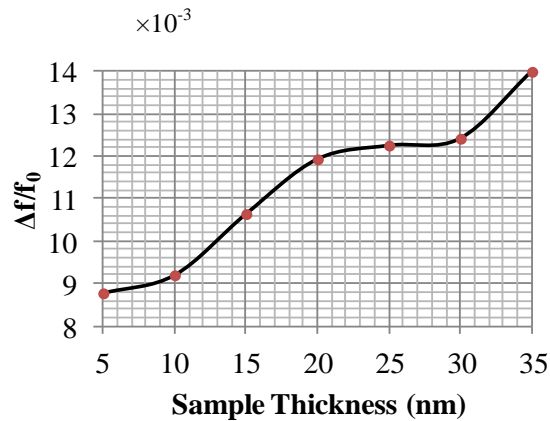


Fig 8. Frequency shifts with changing nano layer thicknesses. These gaps are filled with nano layers of different dielectric constants (material permittivity) as compared to its absence. The testing results are summarized in Fig 8. The shift in resonant frequency increases somehow linearly as the nano layers of different dielectric constants are loaded on the surface of sensor across gap areas. This behavior reveals that further change in dielectric constants leads to prominent shifts.

CONCLUSION

The reported sensor works well for sensing of nano layers of different dielectric materials. Sharp resonance magnitudes effectively distinguishes loading of nano layers of different dielectric constants. The metamaterial structure is so flexible in terms of circuit functionality that it can be used in number of applications related to the direct sensing of various biochemicals and biological substance detection like lipopolysaccharide, squamous cell carcinoma Antigen, cancer antigens, myelin Proteins biomarkers, Septicemia poisoning bacteria etc. Resonant behavior at 7.5 THz enables the reported sensor device to be used in widely available antenna-sensor and filter related applications. It is believed that the sensing performance of proposed sensor can greatly be enhanced by integration with graphene layer.

The surface electric field distribution is affected and the changes itself. Such a change causes a resulting change in the refractive index that also shifts the magnitude of transmission coefficient parameter of the sensor in terms of S_{21} magnitude.

References

[1] Pendry, J.B., Holden, A.J., Robbins, D.J. and Stewart, W.J., "Magnetism from conductors and enhanced nonlinear phenomena", *IEEE Transaction on Microwave Theory Tech*, **47**(11): 2075–2084 (1999).

[2] Shelby, R.A., Smith, D.R. and Schultz, S., "Experimental verification of a negative index of refraction", *Science*, **292**(5514): 77–79 (2001).

[3] Li, J. and Huang, Y., "Time-Domain Finite Element Methods for Maxwell's Equations in Metamaterials", *Springer Series in Computational Mathematics*, **43**: 1-17 (2012).

[4] Chen, H., Ran, L., Huangfu, J., Zhang, X. and Chen, K., "Left-handed materials composed of only S-shaped resonators", *Physics Review E*, **70**(5): 057605(1)-(4), (2004).

[5] Wu, B. I., Wang, W., Pacheco, J., Chen, X., Grzegorzczak, T. and Kong, J. A., "A study of using metamaterials as antenna substrate to enhance gain" *PIER*, **51**: 295-328, (2005).

[6] Ekmekci, E. and G. Turhan-Sayan, "Investigation of permittivity and permeability for a novel V-shaped metamaterial using simulated S-parameters" *Proceedings of 5th International Conference on Electrical and Electronics Engineering*, Bursa, Turkey, (December, 2007).

[7] Naeem, N., Ismail, A., Alhawari, H., Reda, A. and Mahdi, M. A., "Terahertz Dielectric Sensor Based on Novel Hexagon Meta-Atom Cluster", *Applied Computational Electromagnetics Society Journal*, **30**(9): 996-1002, (2015).

[8] Sabah, C., "tunable metamaterial design composed of triangular split ring resonator and wire strip for S and C microwave bands", *PIER-B*, **22**: 341-357, (2010).

[9] Naeem, N., Ismail, A., Alhawari, A. R. H. and Mahdi, M. A., "Subwavelength negative index planar terahertz metamaterial arrays using spiral split ring resonators for near field sensing", *International Journal of Applied Electromagnetics and Mechanics*, **47**(3), 827-836, (2015).

[10] Choudhury, B., Menon A. and Jha, R. M., "Active Terahertz Metamaterial for Biomedical Applications", *Springer Singapore*, 1-41, (2016). Doi:10.1007/978-981-287-793-2_1

[11] Aznar, F., Gil, M., Bonache, J., Garcia-Garcia, J. and Martin, F., "Metamaterial transmission lines based on broadside coupled spiral resonators", *Electronics Letters*, **43**(9): 530-532, (2007).

[12] Baena, J. D., Marques, R., Medina, F. and Martel, J. Artificial magnetic metamaterial design by using spiral resonators. *Physical review B*, **69**(1): 014402(1-5), (2004).

[13] Withawat W. and Abbott, D., "Metamaterials in the Terahertz Regime", *Ieee photonics journal*, **1**(2): 99-118, (2009).

[14] Ekmekci, E. and Turhan-Sayan, G., "Comparative investigation of resonance characteristics and electrical size of the double-sided SRR, BC-SRR and conventional SRR type metamaterials for varying substrate parameters", *Progress In Electromagnetics Research B*, **12**: 35-62, (2009).

[15] Smith, D. R., Vier, D. C., Koschny, T. and Soukoulis, C. M., "Electromagnetic parameter retrieval from inhomogeneous metamaterials", *Physical review E* **71**, 036617, (2005).